Proceedings of the 17th World Congress
The International Federation of Automatic Control
Seoul, Korea, July 6-11, 2008

Extended Luenberger Observer for a MIMO Nonlinear Nonholonomic System

Edgar Ergueta * **Robert Seifried** ** **Roberto Horowitz** *
Masayoshi Tomizuka *

* *Mechanical Engineering Department, University of California, Berkeley, CA 94720, USA (e-mails: eergueta@me.berkeley.edu; horowitz@me.berkeley.edu; tomizuka@me.berkeley.edu)*
** *Institute of Engineering and Computational Mechanics, University of Stuttgart, 70550 Stuttgart, Germany (e-mail: seifried@itm.uni-stuttgart.de)*

Abstract: State of the art high speed color printers require sheets being accurately positioned as they arrive to the image transfer station (ITS). This goal has been achieved by constructing a steerable nips mechanism, which is located upstream from the ITS. This mechanism consists of two rollers which not only rotate to advance the paper along the track, but also steer the paper in the yaw direction. A recently developed nonlinear control strategy for the position of the sheet is briefly reviewed. The core of this paper focuses on the addition of a nonlinear observer used to estimate the longitudinal, lateral, and angular positions of a sheet, by detecting its motion along two of its perpendicular sides. The success of the approach presented is corroborated through simulations, in which the estimates from the extended Luenberger observer designed are used on a nonlinear feedback control strategy.

1. INTRODUCTION

State of the art paper path control currently requires the sheets to be accurately positioned as they arrive to the image transfer station (ITS). This is achieved by using a registration device, which not only corrects for longitudinal, lateral and angular errors, but also delivers the sheet on time to the ITS. However, current designs cannot correct position errors at high speeds or cannot do it without marking the page. In Sanchez et al. [2006], a new mechatronic solution to this problem is presented using the steerable nips device depicted in Fig. 1 (US Patent Number 6,634,521), which consists on two rollers separated by a fixed distance, which can both rotate and steer.

The control strategy used in Sanchez et al. [2006] to correct errors in the lateral, longitudinal and skew directions of the sheet is based on linearization by state feedback (Sastry [1999]) with the addition of internal loops for the local control of the process direction velocity (along vector $\underline{v}$ in Fig. 1) and steering position of the rollers. Ergueta et al. [2007] presents a methodology for the calibration of the controller gains.

Sanchez et al. [2006], however, estimates the lateral, longitudinal, and skew positions of the sheet through the use of an open-loop observer, based on the kinematics relations of the system and the direct measurement of the angular position. In this paper we use a lateral laser sensor and a process direction sensor (see Fig. 1) to detect the motion of two perpendicular edges of the sheet. These measurements are in term used in a closed-loop extended Luenberger observer, which is based on the work by Bestle and Zeitz [1983] and Birk and Zeitz [1988]. Such an observer is an extension to the normal form observer developed by

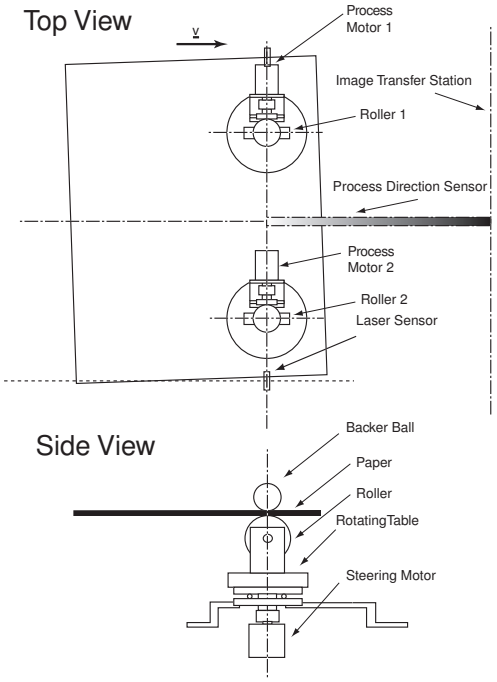

Fig. 1. Schematic of steerable nips Fixture

Krener and Isidori [1983], where some of the conditions required by the latter are relaxed.

Even though there is not a general equivalent to the separation principle for nonlinear systems, we first design a control law assuming the state vector can be measured, then we construct an observer, whose error dynamics converge to a specified bound within a certain time, and finally we apply the previously determined controller using

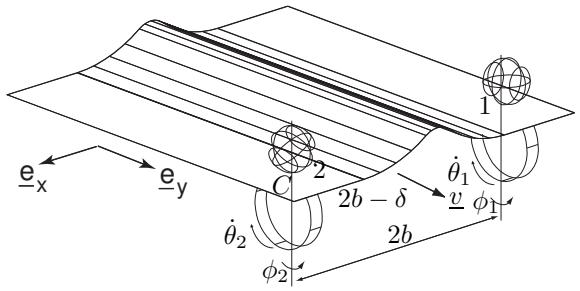

Fig. 2. Steerable nips with paper buckle

observer states, similar to the technique proposed by Vidyasagar [1980].

The remainder of this paper is organized as follows. Section 2 briefly describes the steerable nips and mathematical model of the system. Section 3 shows the control strategy used. Then, section 4 presents a summary of the extended Luenberger observer for SISO and MIMO systems. Section 5 shows an application of this observer for the steerable nips mechanism. Conclusions are stated in Section 6.

2. STEERABLE NIPS MECHANISM

The steerable nips mechanism has been designed so that it can correct for lateral errors without inflicting any damage on the paper. This is possible by independently steering two rollers, which are underneath a backer ball. Each roller is driven by a servo motor attached to a rotating table, which is in turn steered by another servo motor through a coupling. This mechanism has been built and is described in Sanchez et al. [2004]. As we can see in Fig. 2, the page moves along a flat surface (not shown for clarity purposes) in the direction of the arrow labeled $\underline{v}$, which henceforth will be referred as the process direction of the paper, and passes between the backer balls and the rollers.

The two rollers, located at points 1 and 2, are separated by a fixed distance $2b$. The space-fixed coordinates of the system (x, y, ϕ, δ) locate the leading right corner of the sheet, point C, which will be used to track the position of the page. Note that x and y are the lateral and longitudinal positions, respectively, ϕ is the angular position, and δ is the amount of buckling along the sheet, which is the difference between the distance separating points 1 and 2, as measured along the paper $(2b-\delta)$ and along the straight line $(2b)$, as shown in Fig. 2. Also note that a negative δ represents the amount of buckle on a sheet whereas a positive δ occurs when the paper stretches, which needs to be avoided at all times. Also note that the origin $(0, 0)$ of the space-fixed frame is located in the middle of points 1 and 2. Furthermore, $\dot{\theta}_i$ $(i = 1, 2)$ represent the angular velocity of the rollers in the direction parallel to the sheet, and ϕ_i $(i = 1, 2)$ represents their angular position in the direction perpendicular to the sheet.

Note also that the steerable nips mechanism is a four-input, four-output nonlinear system with four nonholonomic constraints. These constraints come from non slip conditions on the rollers, and local velocities (of the paper) being zero in the direction perpendicular to the rotation of the rollers. Additional details on these constraints can be found in Sanchez et al. [2004]. The kinematic model of the system is derived so that these four nonholonomic constraints are satisfied at all times. This model, whose complete derivation can be found in Sanchez et al. [2006], is represented by the following equations:

$$\dot{x} = r_1(\sin\phi_1 - \frac{y}{2b+\delta}\cos\phi_1)\dot{\theta}_1 + \frac{r_2 y}{2b+\delta}\cos\phi_2\dot{\theta}_2 \quad (1)$$

$$\dot{y} = r_1\cos\phi_1(\frac{x+b}{2b+\delta} - 1)\dot{\theta}_1 - \frac{r_2(x+b)}{2b+\delta}\cos\phi_2\dot{\theta}_2 \quad (2)$$

$$\dot{\phi} = \frac{1}{2b+\delta}(r_1\cos\phi_1\dot{\theta}_1 - r_2\cos\phi_2\dot{\theta}_2) \quad (3)$$

$$\dot{\delta} = r_2\sin\phi_2\dot{\theta}_2 - r_1\sin\phi_1\dot{\theta}_1 \quad (4)$$

As mentioned in Sanchez et al. [2006], a simple model that adequately described both the process direction and steering actuator dynamics, reads

$$\ddot{\theta}_i + \alpha_{pi}\dot{\theta}_i = \beta_{pi}V_{pi}; \quad (i = 1, 2) \quad (5)$$

$$\ddot{\phi}_i + \alpha_{si}\dot{\phi}_i = \beta_{si}V_{si}; \quad (i = 1, 2) \quad (6)$$

where V_i is the voltage input to the motor, and α_i and β_i are coefficients that depend on the inertias and rotational viscous damping coefficients of the different components of the steer-able nips mechanism. Subindexes p and s stand for process direction and steering actuators, respectively, and subindex i corresponds to each of the two rollers.

Finally, using Eqs.(1)-(6) and letting $\underline{x} = [x \;\; y \;\; \phi \;\; \delta \;\; \phi_1 \;\; \phi_2 \;\; \dot{\theta}_2 \;\; \dot{\theta}_2 \;\; \dot{\phi}_1 \;\; \dot{\phi}_2]^T$ be the state vector, we obtain the following state space representation:

$$\frac{d}{dt}\begin{pmatrix} x \\ y \\ \phi \\ \delta \\ \phi_1 \\ \phi_2 \\ \dot{\theta}_1 \\ \dot{\theta}_2 \\ \dot{\phi}_1 \\ \dot{\phi}_2 \end{pmatrix} = \begin{pmatrix} f_x(\underline{x}) \\ f_y(\underline{x}) \\ f_\phi(\underline{x}) \\ f_\delta(\underline{x}) \\ \dot{\phi}_1 \\ \dot{\phi}_2 \\ -\alpha_{p1}\dot{\theta}_1 \\ -\alpha_{p2}\dot{\theta}_2 \\ -\alpha_{s1}\dot{\phi}_1 \\ -\alpha_{s2}\dot{\phi}_2 \end{pmatrix} + \begin{pmatrix} 0 & 0 & 0 & 0 \\ 0 & 0 & 0 & 0 \\ 0 & 0 & 0 & 0 \\ 0 & 0 & 0 & 0 \\ 0 & 0 & 0 & 0 \\ 0 & 0 & 0 & 0 \\ \beta_{p1} & 0 & 0 & 0 \\ 0 & \beta_{p2} & 0 & 0 \\ 0 & 0 & \beta_{s1} & 0 \\ 0 & 0 & 0 & \beta_{s2} \end{pmatrix} \begin{pmatrix} V_{p1} \\ V_{p2} \\ V_{s1} \\ V_{s2} \end{pmatrix} \quad (7)$$

$$\underline{y} = \begin{pmatrix} x & y & \phi & \delta \end{pmatrix}^T \quad (8)$$

where $f_x(\underline{x})$, $f_y(\underline{x})$, $f_\phi(\underline{x})$, and $f_\delta(\underline{x})$ are given by Eqs.(1)-(4), respectively.

3. CONTROL STRATEGY

The block diagram of the control system is shown in Fig. 3. Here, the *Plant* is represented by the kinematic equations (1)-(4), the process direction actuators, P_{p1} and P_{p2}, by Eq.(5), and the steering actuators, P_{s1} and P_{s2}, by Eq.(6). Furthermore, if we differentiate Eq.(8) twice, we obtain

$$\ddot{\underline{y}} = \underline{m}(\underline{x}) + N(\underline{x}) \begin{bmatrix} \ddot{\theta}_1 \\ \ddot{\theta}_2 \\ \dot{\phi}_1 \\ \dot{\phi}_2 \end{bmatrix} \quad (9)$$

where $m(\underline{x})$ is a 4×1 vector and $N(\underline{x})$ is a 4×4 matrix, both of which depend nonlinearly on the system states. Thus, we design the nonlinear feedback control law, C_{FBL}, which is based on feedback linearization, and is given by:

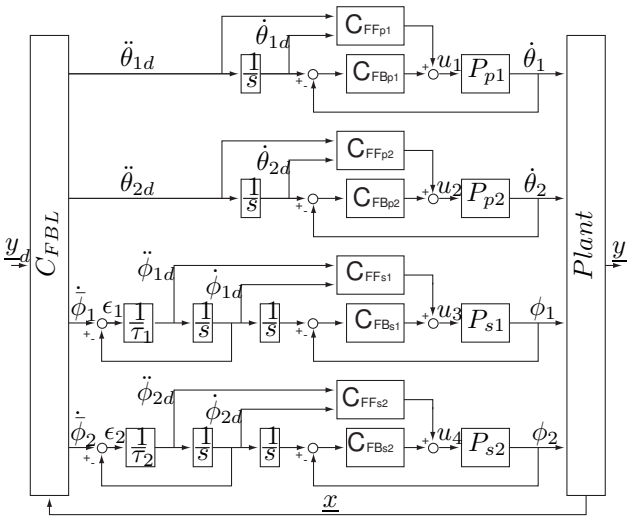

Fig. 3. System block diagram

$$\begin{bmatrix} \ddot{\theta}_{1d} \\ \ddot{\theta}_{2d} \\ \dot{\phi}_{1d} \\ \dot{\phi}_{2d} \end{bmatrix} = N^{-1}(\underline{x})(\underline{v} - \underline{m}(\underline{x})) \tag{10}$$

Note that we also use a feedback plus feedforward control strategy to control locally the velocity of the process direction motors:

$$C_{FB_{pi}}(s) = \eta_{pi} + \frac{\gamma_{pi}}{s};\ C_{FF_{pi}}(s) = \frac{1}{\beta_{pi}}(1 + \frac{\alpha_{pi}}{s});\ (i = 1, 2) \tag{11}$$

where η_{pi} and γ_{pi} are the PI controller gains, and α_{pi} and β_{pi} are defined in Eq. (5) for $i = 1, 2$. We use a similar strategy to control locally the position of the steering actuators:

$$C_{FB_{si}}(s) = \eta_{si} + \gamma_{pi}s;\ C_{FF_{si}}(s) = \frac{1}{\beta_{si}}(1 + \frac{\alpha_{si}}{s});\ (i = 1, 2) \tag{12}$$

where η_{si} and γ_{si} are the PD controller gains, and α_{si} and β_{si} are defined in Eq. (6) for $i = 1, 2$. As shown in Fig. 3, in order to use feedforward for steering position control, we need to generate the steering acceleration estimate, $\ddot{\phi}_{id}$, through the use of a first order filter with gain τ_i $(i = 1, 2)$; if τ_i is sufficiently small, the value of $\dot{\phi}_{id}$ will be very close to that of $\dot{\bar{\phi}}_i$. In order to ensure that the state errors converge to zero Ergueta et al. [2007] shows that vector $\underline{v}$ needs to be defined as

$$\underline{v} = \begin{pmatrix} \ddot{x}_d + (K_x + \lambda_x)(\dot{x_d} - \dot{x}) + K_x\lambda_x(x_d - x) \\ \ddot{y}_d + (K_y + \lambda_y)(\dot{y_d} - \dot{y}) + K_y\lambda_y(y_d - y) \\ \ddot{\phi}_d + (K_\phi + \lambda_\phi)(\dot{\phi_d} - \dot{\phi}) + K_\phi\lambda_\phi(\phi_d - \phi) \\ \ddot{\delta}_d + (K_\delta + \lambda_\delta)(\dot{\delta_d} - \dot{\delta}) + K_\delta\lambda_\delta(\delta_d - \delta) \end{pmatrix} \tag{13}$$

where all gains, K, λ, in Eq.(13) need to be positive. Note that the success of this control strategy depends on the invertibility of matrix $N(x)$. In Sanchez et al. [2006] it is shown that this matrix is invertible as long as the sheet is always moving in the process direction. Furthermore, a methodology to obtain the controller gains required to correct the position and amount of buckling of a finite-length page with any predetermined initial errors is presented in Ergueta et al. [2007], where simulation and experimental results are also shown.

4. EXTENDED LUENBERGER OBSERVER THEORY

One approach for nonlinear observer design, is the normal form observer (Krener and Isidori [1983] and Bestle and Zeitz [1983]). A normal form observer has linear error dynamics in the coordinates of the observer normal form. The design of a normal form observer requires the transformation into observer normal form and output injection. This approach, also called exact error linearization, is dual to feedback linearization (Isidori [1995], Sastry [1999]). However, the transformation to observer normal form requires the solution of partial differential equations, whose solvability conditions are very strict. The extended Luenberger observer is a modification of the normal form observer, and due to Bestle and Zeitz [1983] and Birk and Zeitz [1988]. This type of observer has a typical Luenberger structure and is based on an extended Jacobian linearization of the error dynamics in coordinates of the observer normal form. The conditions for the use of the extended Luenberger observer are less strict. The following summarizes briefly the underlying theory for the extended Luenberger observer.

4.1 Local Observability and Observer Normal Form

Let us first consider the following nonlinear unforced single-output system

$$\dot{\underline{x}} = \underline{f}(\underline{x}), \quad y = h(\underline{x}) \tag{14}$$

where the smooth vector fields $\underline{f} : M \to I\!R^n$ and smooth output function $h : M \to I\!R$ are defined on the open set $M \subset I\!R^n$. The observability map $q(\underline{x})$ and the observability matrix $Q(\underline{x})$ are given by

$$q(\underline{x}) = \begin{pmatrix} h(\underline{x}) \\ L_f h(\underline{x}) \\ \vdots \\ L_f^{n-1} h(\underline{x}) \end{pmatrix}; \quad Q(\underline{x}) = \frac{\partial q(\underline{x})}{\partial \underline{x}} = \begin{pmatrix} dh(\underline{x}) \\ dL_f h(\underline{x}) \\ \vdots \\ dL_f^{n-1} h(\underline{x}) \end{pmatrix} \tag{15}$$

Therein L_f^i denotes the i^{th} Lie-derivative, and the differential of the Lie derivative is denoted by dL_f^i. System (14) is said to be locally observable if the $n \times n$ observability matrix $Q(\underline{x})$ has rank n for all x within a local region.

The observer design problem is simplified if system (14) can be transformed into observer normal form by the diffeomorphic coordinate transformation

$$\underline{x}^* = F^{-1}(\underline{x}), \quad \underline{x} = F(\underline{x}^*) \tag{16}$$

As proven in Isidori [1995], the Jacobian matrix of the transformation, computed in original coordinates reads

$$\frac{\partial F}{\partial \underline{x}^*}\Big|_{\underline{x}^* = F^{-1}(\underline{x})} = \left[\underline{s}(\underline{x}),\ ad_{-f}\underline{s}(\underline{x}),\ \ldots,\ ad_{-f}^{n-1}\underline{s}(\underline{x})\right] \tag{17}$$

where $ad_{-f}^i \underline{s}(\underline{x})$ is the i^{th} Lie-bracket and vector $\underline{s}(\underline{x})$ is given by the last column of the inverse observability matrix,

$$\underline{s}(\underline{x}) = Q^{-1}[0.....0\ 1]^T \tag{18}$$

From this transformation, the observer normal form is

$$\dot{\underline{x}}^* = E\underline{x}^* + \underline{\alpha}(y); \quad y = x_n^* \tag{19}$$

where E is a $n \times n$ matrix with 1 entries on the first lower sub-diagonal, while all other elements are 0. Note, that the

output only depends on x_n^*. In these new coordinates an observer can be constructed in such a way, that it posses linear error dynamics. This yields the so called *normal form observer*. However, the transformation into observer normal form requires:

(1) $rank(Q) = n$
(2) $\left[ad^i_{-f}\underline{s}(\underline{x}), ad^j_{-f}\underline{s}(\underline{x})\right] = 0, \quad i,j = 0,1,\ldots,n-1$

Not only is the second condition very strict, but even if both conditions are met, the transformation involves the solution of a set of partial differential equations, which is difficult to obtain even for low order systems.

4.2 Extended Luenberger observers for SISO systems

The extended Luenberger observer is based on the typical Luenberger observer structure,

$$\dot{\underline{\hat{x}}} = f(\underline{\hat{x}}) + \underline{l}(\underline{\hat{x}})[y - h(\underline{\hat{x}})] \tag{20}$$

where $\underline{\hat{x}}$ is the observer state vector and $\underline{l}(\underline{\hat{x}})$ is the observer gain. In the coordinates of the observer normal form, observer (20) is given by

$$\dot{\underline{\hat{x}}}^* = E\underline{\hat{x}}^* + \underline{\alpha}(\hat{x}_n^*) + \underline{l}^*(\underline{\hat{x}}^*)[x_n^* - \hat{x}_n^*] \tag{21}$$

where the observer gains in the original and normal coordinates are related by

$$\underline{l}(\underline{\hat{x}}) = \left(\frac{\partial F(\underline{\hat{x}}^*)}{\partial \underline{\hat{x}}^*}\underline{l}^*(\underline{\hat{x}}^*)\right)\Big|_{\underline{\hat{x}}^* = F^{-1}(\underline{\hat{x}})} \tag{22}$$

Thus, the error dynamics in normal form coordinates reads

$$\dot{\underline{e}}^* = E\underline{e}^* + \underline{\alpha}(x_n^*) - \underline{\alpha}(\hat{x}_n^*) - l^*(\underline{\hat{x}}^*)[x_n^* - \hat{x}_n^*] \tag{23}$$

where $\underline{e}^* = \underline{x}^* - \underline{\hat{x}}^*$ is the observer error. Then, an extended Jacobian linearization of $\underline{\alpha}(x_n^*) - \underline{\alpha}(\hat{x}_n^*)$ in Eq.(23) around the observer trajectory $\hat{x}_n^*$ yields for small $e_n^* = x_n^* - \hat{x}_n^* \ll 1$ the following error dynamics

$$\dot{\underline{e}}^* = E\underline{e}^* - \left[\frac{\partial \underline{\alpha}}{\partial \hat{x}_n^*} - \underline{l}^*(\underline{\hat{x}}^*)\right] e_n^* + O^2(e_n^*) \tag{24}$$

Using the special choice for the observer gains

$$\underline{l}^*(\underline{\hat{x}}^*) = \frac{\partial \underline{\alpha}}{\partial \hat{x}_n^*} + \underline{p} \tag{25}$$

and neglecting higher order terms in Eqn.(24) we obtain the following approximated linear and time-invariant error dynamics

$$\dot{\underline{e}}^* = E\underline{e}^* + \underline{p}e_n^* \tag{26}$$

whose poles can be placed arbitrarily by an appropriate choice of the coefficients $\underline{p} = [p_0, p_1, \ldots, p_{n-1}]^T$ of its characteristic polynomial.

Finally, from Eqs.(17), (22), (25), and the following relation proven in Bestle and Zeitz [1983],

$$\frac{\partial F(\underline{\hat{x}}^*)}{\partial \underline{\hat{x}}^*}\frac{\partial \underline{\alpha}}{\partial \hat{x}_n^*} = ad^n_{-f}\underline{s}(\underline{\hat{x}}) \tag{27}$$

the observer gain in the original coordinate frame is

$$\underline{l}(\underline{\hat{x}}) = \left[p_0 ad^0_{-f} + p_1 ad^1_{-f} + \ldots + p_{n-1}ad^{n-1}_{-f} + ad^n_{-f}\right] \circ \underline{s}(\underline{\hat{x}}) \tag{28}$$

Note that the computation of the observer gain in Eq.(28) for the extended Luenberger observer (20) can be directly performed in original coordinates using symbolic programs such as *Mathematica*. From Eqs.(18) and (28) also note that matrix $Q(\underline{x})$ needs to have full rank, but condition (2) in section 4.1 does not need to be satisfied.

4.3 Extended Luenberger observers for MIMO systems

Since the steerable nips mechanism is a MIMO system, it is necessary to use an extension to the extended Luenberger observer, which is given by Birk and Zeitz [1988]. For a system with output $\underline{y} = \underline{h}(\underline{x}) = (h_1(\underline{x}), \ldots, h_m(\underline{x}))^T$, the observability map is given by

$$q(\underline{x}) = \left(h_1, \ldots, L_f^{m_1-1}h_1, \ldots, h_m, \ldots, L_f^{m_m-1}h_m\right)^T \tag{29}$$

where the observability indices satisfy $m_1 + \ldots + m_m = n$. The system is locally observable if the observability matrix $Q(\underline{x})$ resulting from Eqn. (29) has rank n. Vector $\underline{s}_{m_i}$ is the k^{th} vector of the inverse observability matrix, where $k_i = \sum_{j=1}^{i} m_j$. In the observer design process the system is decomposed into m decoupled subsystems. The dimensions of the subsystems are given by the observability indices m_i. The desired observer error dynamics of the i^{th} subsystem is described by the characteristic polynomial $a_i(\lambda) = p_{i0} + p_{i_1}\lambda + \ldots + p_{i_{m_i-1}}\lambda^{m_i-1} + \lambda^{m_i}$. Then, as in the SISO case, the observer gain matrix L reads in original coordinates

$$L(\underline{\hat{x}}) = \left[a_1(ad_{-f}) \circ \underline{s}_1, \ \ldots, \ a_m(ad_{-f}) \circ \underline{s}_m\right] \cdot B^{-1} \tag{30}$$

where matrix B (see Roebenack [2004]) is defined by

$$B = \frac{\partial \underline{h}(\underline{\hat{x}})}{\partial \underline{\hat{x}}} \cdot \left[ad_{-f}^{m_1-1}, \ldots, ad_{-f}^{m_m-1}\right] \tag{31}$$

It should be noted that the symbolic computations can be greatly simplified by scaling vectors $\underline{s}_i$ appropriately (Birk and Zeitz [1988]).

Despite the fact that input $\underline{u}$ occurs in the observer problem of controlled systems, the presented overview of the extended Luenberger observer is restricted to unforced systems. A common approach to handle system with inputs is to assume that the inputs are constant in the design process and then their values are constantly updated in the implementation. This approach can be assumed to be valid, as long as the inputs do not vary strongly, such us in the case of the steerable nips system. If this is not the case, the inputs have to be considered explicitly in the design of the extended Luenberger observe as proposed by Birk and Zeitz [1988].

5. OBSERVER DESIGN

In this section the observer described in the previous section will be used in combination to the control strategy described in section 3. Before engaging into this task, let us first set up our observer problem.

In order to determine the position, orientation, and the amount of buckling of the sheet, it is required to measure some of the system states and estimate others. Each of the motors used has a built-in encoder, which let us have measurements for angular positions. Angular velocities are also obtained through numerical differentiation of position due to the high resolution of the encoders and the fast

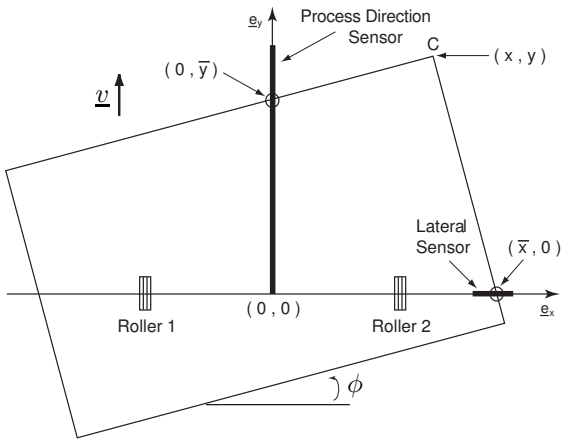

Fig. 4. Geometry for sheet measurements

sampling rate. As seen in Fig. 1, in order to detect a point of the lateral edge of the sheet, a laser sensor is located on the right hand side of the nips section along the line connecting the two rollers (at $y = 0$); this sensor produces measurement $\bar{x}$. Furthermore, we also use a long sensor located between the rollers (at $x = 0$) to detect a point of the leading edge of the sheet; this sensor produces measurement $\bar{y}$. Further details on the sensor scheme can be found in Sanchez et al. [2006]. By looking at Fig. 4 we can write $\bar{x}$ and $\bar{y}$ in terms of the system states as

$$\underline{y} = h(\underline{x}) \equiv \begin{pmatrix} \bar{x} \\ \bar{y} \end{pmatrix} = \begin{pmatrix} x + y\tan\phi \\ y - x\tan\phi \end{pmatrix} \tag{32}$$

Furthermore, since we can also measure states ϕ_1, ϕ_2, $\dot{\theta}_1$, $\dot{\theta}_2$, $\dot{\phi}_1$, and $\dot{\phi}_2$ through encoders, we do not need to estimate them. Thus, we should look at a reduced order observer that only estimates x, y, ϕ, and δ, using Eqs.(1)-(4) as state equations, considering the other states from Eq.(7) as inputs, and taking Eq.(32) as the available measurements. Let us then define the observer states by $\underline{\hat{z}} = (\hat{x}\ \hat{y}\ \hat{\phi}\ \hat{\delta})^T$ and the observer inputs by $\underline{\nu} = (\phi_1\ \phi_2\ \dot{\theta}_1\ \dot{\theta}_2)^T$.

Now, proceeding in a similar manner as in section 4 we can obtain the observability matrix by finding the Lie derivatives of each of the two measurements. Such a matrix is given by,

$$Q(\underline{x}) = \begin{pmatrix} 1 & \tan\phi & \dfrac{y}{\cos^2\phi} & 0 \\ Q_{21} & Q_{22} & Q_{23} & Q_{24} \\ -\tan\phi & 1 & -\dfrac{x}{\cos^2\phi} & 0 \\ Q_{41} & Q_{42} & Q_{43} & Q_{44} \end{pmatrix} \tag{33}$$

where

$$\begin{aligned}
Q_{21} &= \frac{(r_1\dot{\theta}_1\cos\phi_1 - r_2\dot{\theta}_2\cos\phi_2)\tan\phi}{2b+\delta} \\
Q_{22} &= \frac{(r_1\dot{\theta}_1\cos\phi_1 - r_2\dot{\theta}_2\cos\phi_2)\tan^2\phi}{2b+\delta} \\
Q_{23} &= -\frac{1}{2b+\delta}\Big(\frac{1}{\cos^2\phi}(r_1\dot{\theta}_1\cos\phi_1(b+\delta-x-2y\tan\phi) \\
&\quad + r_2\dot{\theta}_2\cos\phi_2(b+x+2y\tan\phi))\Big) \\
Q_{24} &= -\frac{1}{(2b+\delta)\cos^2\phi}(r_1\dot{\theta}_1\cos\phi_1 - r_2\dot{\theta}_2\cos\phi_2) \\
&\quad \times((b+x)\cos\phi + y\sin\phi\tan\phi)
\end{aligned} \tag{34}$$

$$\begin{aligned}
Q_{41} &= -\frac{(r_1\dot{\theta}_1\cos\phi_1 - r_2\dot{\theta}_2\cos\phi_2)\tan^2\phi}{2b+\delta} \\
Q_{42} &= \frac{(r_1\dot{\theta}_1\cos\phi_1 - r_2\dot{\theta}_2\cos\phi_2)\tan\phi}{2b+\delta} \\
Q_{43} &= \frac{1}{(2b+\delta)\cos^2\phi}(-(2b+\delta)r_1\dot{\theta}_1\sin\phi_1 \\
&\quad + r_1\dot{\theta}_1\cos\phi_1(y-2x\tan\phi) - r_2\dot{\theta}_2\cos\phi_2(y-2x\tan\phi)) \\
Q_{44} &= -\frac{1}{2(2b+\delta)}((r_1\dot{\theta}_1\cos\phi_1 - r_2\dot{\theta}_2\cos\phi_2)\frac{1}{\cos^2\phi} \\
&\quad \times(b - x + (b+x)\cos(2\phi) + y\sin(2\phi)))
\end{aligned} \tag{35}$$

By looking at the equations above we can see that matrix $Q(\underline{x})$ becomes singular when $r_1 = r_2$, $\dot{\theta}_1 = \dot{\theta}_2$, and $\phi_1 = \phi_2$, since in that case buckling becomes unobservable. However, since we are interested in correcting the sheet position errors only to within a desired tolerance we minimize the possibility for this to happen. In all other cases matrix $Q(\underline{x})$ has full rank and satisfies the conditions for the extended Luenberger observer. We then find the inverse of $Q(\underline{x})$, and define its second and fourth columns as $\underline{s}_1$ and $\underline{s}_2$, respectively. It follows from Eq.(31) that for the vectors $\underline{s}_1$ and $\underline{s}_2$ used, matrix B is the identity matrix. Therefore we obtain the following observer gain:

$$L(\underline{\hat{x}}) = \left[a_1(ad_{-f}) \circ \underline{s}_1,\ a_2(ad_{-f}) \circ \underline{s}_2\right] \tag{36}$$

where

$$\begin{aligned}
a_1(ad_{-f}) \circ \underline{s}_1 &= p_{01}\underline{s}_1 + p_{11}ad_{-f}\underline{s}_1 + ad^2_{-f}\underline{s}_1 \\
a_2(ad_{-f}) \circ \underline{s}_2 &= p_{02}\underline{s}_2 + p_{12}ad_{-f}\underline{s}_2 + ad^2_{-f}\underline{s}_2
\end{aligned} \tag{37}$$

and where p_{ij} are the design parameters that let us set the eigenvalues of the observer error dynamics at any desired location. The observer dynamics are then given by

$$\dot{\underline{\hat{z}}} = \underline{f}(\underline{\hat{z}}) + L(\underline{\hat{x}})[\underline{y} - \underline{\hat{h}}(\underline{\hat{z}})] \tag{38}$$

where

$$\begin{aligned}
\underline{f}(\underline{\hat{z}}) &= \left(\ f_{\hat{x}}(\underline{\hat{z}},\underline{\nu})\ \ f_{\hat{y}}(\underline{\hat{z}},\underline{\nu})\ \ f_{\hat{\phi}}(\underline{\hat{z}},\underline{\nu})\ \ f_{\hat{\delta}}(\underline{\hat{z}},\underline{\nu})\ \right)^T \\
\underline{\hat{h}}(\underline{z}) &= \left(\ h_1(\underline{\hat{z}})\ \ h_2(\underline{\hat{z}})\ \right)^T
\end{aligned} \tag{39}$$

and where $f_{\hat{x}}(\underline{\hat{z}},\underline{\nu})$, $f_{\hat{y}}(\underline{\hat{z}},\underline{\nu})$, $f_{\hat{\phi}}(\underline{\hat{z}},\underline{\nu})$, and $f_{\hat{\delta}}(\underline{\hat{z}},\underline{\nu})$ are equal to $f_x(\underline{x})$, $f_y(\underline{x})$, $f_\phi(\underline{x})$, and $f_\delta(\underline{x})$ with x, y, ϕ, and δ replaced by $\hat{x}, \hat{y}, \hat{\phi}$, and $\hat{\delta}$, respectively.

Using the controller presented in section 3 and the observer presented in this section we obtain the simulations results shown in Figs. 5 and 6 for the observer errors and the paper state errors, respectively.

For this simulation we chose the observer gains so that the observer error dynamics converge as fast as possible to zero and we designed the controller gains so that we can correct the position of a letter-sized sheet moving at a nominal longitudinal velocity of 0.5m/s along a 20.8cm section, which gives 0.42 seconds of control time. The controller and observer gains used are:

$$\begin{array}{cccc}
K_x = 7.3; & K_y = 13.2; & K_\phi = 7.9; & K_\delta = 6.0 \\
\lambda_x = 60; & \lambda_y = 60; & \lambda_\phi = 60; & \lambda_\delta = 60 \\
\eta_{p1} = 0.14; & \gamma_{p1} = 1.95; & \eta_{p2} = 0.14; & \gamma_{p2} = 1.95 \\
\eta_{s1} = 52.8; & \gamma_{s1} = 6.81; & \eta_{s2} = 52.8; & \gamma_{s2} = 6.81 \\
\tau_1 = 0.0042; & \tau_2 = 0.0013; & p_{01} = 4356; & p_{11} = 132 \\
p_{02} = 4356; & p_{12} = 132 & &
\end{array} \tag{40}$$

As seen in Fig. 5, all observer errors have a transient response with initial peaks, which then converge close to

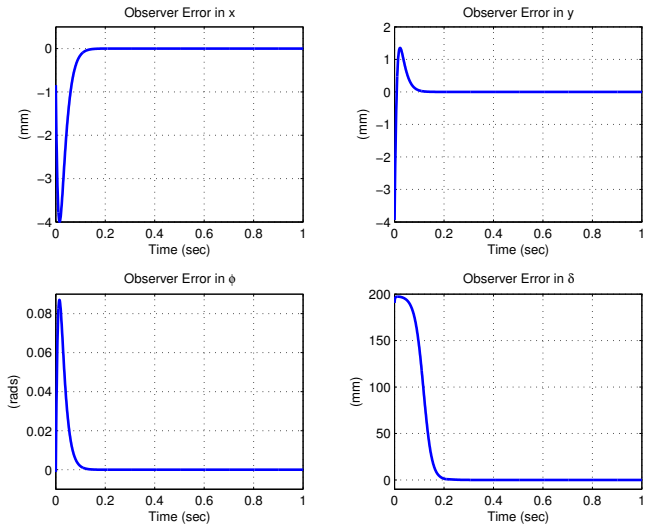

Fig. 5. Observer error dynamics

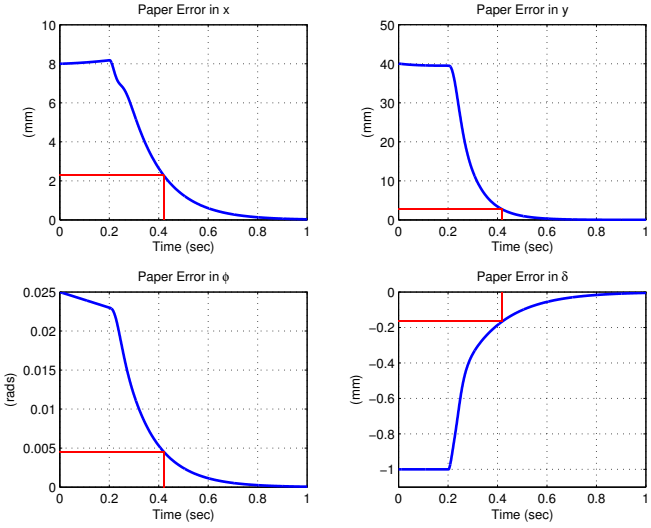

Fig. 6. Paper state errors

zero in about 0.2 seconds. Due to these initial peaks, it was decided that control action will not be used for 0.2 seconds after the page enters the nips section. In other words, we first let the observer errors converge close to zero by letting the page move in open loop, and then the controller is turned on. This strategy can be seen in Fig. 6, where some of the sheet position errors even increase slightly during the first 0.2 seconds. After the initial delay, the controller takes full action and reduces the state errors within the desired tolerance. In particular Fig. 6 shows that we were able to reduce the state errors within the allowed 0.42 seconds from $(x_o, y_o, \phi_o, \delta_o)$ =(8mm,40mm,0.25rad,−1mm) to $(x_f, y_f, \phi_f, \delta_f)$ =(2.3mm,2.7mm,0.0045rad,−0.17mm) with initial observer states of $(\hat{x}_o, \hat{y}_o, \hat{\phi}_o, \hat{\delta}_o)$ = (8.8mm,44mm,0.275rad,−1.1mm), which represent an error of 10 percent of the initial state values.

6. CONCLUSION

In this paper we have presented an innovative design that permits a swifter correction of lateral, longitudinal and angular position errors in a paper path control system for xerographic and printing devices. We accomplished this task by using a mechanism with steerable nips.

We have designed the controller and observer independently from one another. The controller implemented is based on state feedback linearization with inner loops for the local control of the roller rotational velocity and steering position. The reduced order observer designed is based on the extended Luenberger observer for MIMO systems.

Simulation results show that, by using the presented nonlinear observer and nonlinear controller, it is possible to correct position errors of the sheet while the page is continuously moving in the process direction with a predefined desired longitudinal velocity.

In the near future we plan to implement the proposed observer in the experimental setup that has been already built and is described in Sanchez et al. [2006].

ACKNOWLEDGEMENTS

This work was supported by the National Science Foundation under Grant CMS 0301719 and by financial support and collaboration from Xerox Corporation. In particular, the authors thank Dr. Martin Krucinski for his numerous critical remarks. The financial support by DAAD (German Academic Exchange Service) to the second author is greatly acknowledged.

REFERENCES

D. Bestle and M. Zeitz. Canonical form observer design for non-linear time-invariant systems. *International Journal of Control*, Vol. 38, No. 2, pages 419-431, 1983.

J. Birk and M. Zeitz. Extended Luenberger observer for non-linear multivariable systems. *International Journal of Control*, Vol. 47, No. 6, pages 1823-1835, 1988.

E. Ergueta, R. Sanchez, R. Horowitz, and M. Tomizuka. Full sheet control through the use of steer-able nips. Accpeted for publication at the ASME International Mechanical Engineering Congress and Exposition, Seattle, Washington, November 11-15, 2007.

A. Isidori. *Nonlinear Control Systems*. Springer, 1995.

A. Krener and A. Isidori. Linearization by output injection and nonlinear observers. *Systems & Control Letters*, Vol. 3, pages 47-52, 1983.

K. Roebenack. Computation of the observer gains for extended Luenberger observer using automatic differentiation. *IMA Journal of Mathematical Control and Information*, Vol. 21, pages 33-47, 2004.

R. Sanchez, R. Horowitz, M. Tomizuka. Paper sheet control using steerable nips. *American Control Conference Proceedings*, pages 482-487, Boston, Massachusetts, June 30-July 2, 2004.

R. Sanchez, E. Ergueta, B. Fine, R. Horowitz, M. Tomizuka, and M. Krucinski. A mechatronic approach to full sheet control using steer-able nips. *4th IFAC Symposium in Mechatronic Systems*, Heidelberg, Germany, September 12-15, 2006.

S.S. Sastry. *Nonlinear Systems: Analysis, stability, and Control*. Springer, 1999.

M. Vidyasagar. On the stabilization of nonlinear systems using state detection. *IEEE Transactions on Automatic Control*, Vol. AC-25, No. 3, pages 504-509, June 1980.